Published Online: 2026 February 1

Research Article

Dual TYK2/JAK1 Inhibition by Brepocitinib Reprograms Synoviocyte Pathobiology: Mechanistic Insights Into Targeted Therapy for Rheumatoid Arthritis

Umar Saeed [1, 2, *], Zahra Zahid Piracha [3, 4], Andromeda M. Nauli [5], Surya M. Nauli [6, **]

[1] University College, Korea University, Seoul 02418, Republic of KOREA (South KOREA)
[2] Clinical and Biomedical Research Center (CBRC), Foundation University School of Health Sciences (FUSH), Foundation University Islamabad (FUI), Islamabad, Pakistan
[3] Széchenyi István University, Győr, Hungary
[4] Institute of Graduate Studies and Research, Cyprus International University, Nicosia, Cyprus
[5] Department of Biomedical Sciences, School of Medicine, Western Michigan University Homer Stryker, Kalamazoo, USA
[6] Department of Biomedical and Pharmaceutical Sciences, Chapman University, Irvine, United States

[*] ***Corresponding Author:*** University College, Korea University, Seoul 02418, Republic of KOREA (South KOREA). Email: usaeed@chapman.edu
[**] ***Corresponding Author:*** Department of Biomedical and Pharmaceutical Sciences, Chapman University, Irvine, United States. Email: nauli@chapman.edu

Received: 2 September, 2025; **Revised:** 8 November, 2025; **Accepted:** 11 November, 2025

Abstract

Background: Rheumatoid arthritis (RA) is a chronic autoimmune disorder characterized by synovial hyperplasia, persistent inflammation, and joint destruction. Targeted inhibition of intracellular signaling pathways, such as JAK-STAT, has improved RA treatment outcomes, though safety and selectivity remain as concerns. Brepocitinib, a dual TYK2/JAK1 inhibitor, has shown clinical efficacy in the management of autoimmune diseases, yet its mechanistic impact on synoviocytes remains underexplored.

Objectives: To investigate the molecular and functional effects of brepocitinib on MH7A and RA-FLS synoviocytes, a key effector cell type in RA pathogenesis.

Methods: MH7A and RA-FLS cells were treated with brepocitinib (0.5 μM, 1 μM, and 5 μM) for 24 hours. Cell viability was assessed. Western blotting was used to examine phosphorylation of TYK2, JAK1, STAT1/3, and apoptotic markers (BAX, BCL-2, caspase-3). Quantitative PCR and ELISA were performed to evaluate mRNA and protein levels, respectively, of IL-6, TNF-α, and IFN-γ. Wound healing assays measured synoviocyte migration.

Results: Brepocitinib maintained ≥ 85% cell viability across all doses, compared with ~20% viability in doxorubicin-treated controls. At 5 μM, phosphorylation of JAK1 and STAT3 was suppressed by > 80%, while TYK2 and STAT1 inhibition reached ~70%. IL-6 and TNF-α transcripts were reduced by > 80% and IFN-γ by ~70%, with corresponding decreases in secreted cytokines (IL-6: 100 pg/mL to 20 pg/mL; TNF-α: 150 pg/mL to 15 pg/mL; IFN-γ: 41 pg/mL to 11 pg/mL). Brepocitinib shifted the BAX/BCL-2 ratio fourfold in favor of apoptosis and increased cleaved caspase-3 levels to ~80% of maximal response. Functionally, it reduced wound closure from ~75% in controls to ~20% at 5 μM, confirming potent inhibition of synoviocyte migration.

Conclusions: Brepocitinib exerts multi-faceted effects on RA synoviocytes by simultaneously inhibiting inflammatory signaling, suppressing cytokine expression, restoring apoptotic sensitivity, and reducing migratory potential. These findings provide mechanistic support for brepocitinib as a targeted therapeutic agent in RA.

Keywords: Brepocitinib, Rheumatoid Arthritis, TYK2, JAK1, Synoviocytes, JAK-STAT Signaling, Cytokines, Apoptosis, Migration, MH7A, Inflammation, Targeted Therapy

1. Background

Rheumatoid arthritis (RA) is a chronic, systemic autoimmune disorder characterized by persistent synovial inflammation, aberrant immune activation, and progressive destruction of articular cartilage and bone (1). Affecting approximately 0.5 - 1% of the global population, RA not only imposes a significant burden on individual patients but also contributes to substantial socioeconomic costs due to disability and treatment expenses (2). Central to RA pathology is the hyperactivation of fibroblast-like synoviocytes (FLS) — a key stromal cell population within the synovial membrane (3). Under normal conditions, FLS maintain joint homeostasis by producing extracellular matrix components and lubricants (4). However, in RA, these cells adopt an aggressive phenotype, characterized by autonomous proliferation, resistance to apoptosis, and

How to Cite: Saeed U, Zahid Piracha Z, Nauli AM, Nauli SM. Dual TYK2/JAK1 Inhibition by Brepocitinib Reprograms Synoviocyte Pathobiology: Mechanistic Insights Into Targeted Therapy for Rheumatoid Arthritis. Iran J Pharm Res. 2026;25(1):e166019. doi: https://doi.org/10.5812/ijpr-166019

invasive migration into cartilage and bone (3-5). Activated FLS also produce high levels of pro-inflammatory cytokines (e.g., IL-6, TNF-α, IFN-γ) and matrix metalloproteinases, thereby amplifying local inflammation and driving joint destruction (6). The Janus kinase (JAK)-signal transducer and activator of transcription (STAT) signaling axis plays a pivotal role in the orchestration of cytokine signaling in RA (7). In particular, JAK1 and TYK2 mediate intracellular signaling of multiple pro-inflammatory cytokines, such as IL-6, type I interferons, and IL-12/23, which are implicated in RA pathogenesis (8). Consequently, inhibition of JAK family members has emerged as an effective strategy in RA management, as evidenced by FDA approval of tofacitinib (JAK1/3 inhibitor), baricitinib (JAK1/2 inhibitor), and upadacitinib (selective JAK1 inhibitor) in the treatment of RA (9). Brepocitinib is a next-generation, dual TYK2/JAK1 inhibitor that exhibits high potency and selectivity, offering a broader blockade of inflammatory signaling pathways while potentially sparing JAK2-dependent hematopoietic functions (10). Kinase profiling studies have demonstrated that brepocitinib inhibits TYK2 and JAK1 with nanomolar potency (IC_{50} ≈ 22.7 and 16.8 nM, respectively), while showing markedly reduced activity against JAK2 (76.6 nM) and JAK3 (6,490 nM), and minimal inhibition across a panel of > 150 non-JAK kinases (10). These data support its designation as a selective dual TYK2/JAK1 inhibitor. Brepocitinib has shown promising efficacy in clinical trials of psoriatic arthritis, lupus, and hidradenitis suppurativa. However, its mechanistic impact on RA synoviocytes remains largely uncharacterized (10-12). Our findings demonstrate that brepocitinib, at concentrations up to 5 μM, is non-cytotoxic but exerts potent inhibition of the TYK2/JAK1-STAT axis. This suppression translates into a marked reduction in the expression and secretion of pro-inflammatory cytokines, including IL-6, TNF-α, and IFN-γ. Furthermore, brepocitinib reactivates apoptotic pathways in RA synoviocytes by modulating BAX/BCL-2 expression and caspase-3 activation. Functionally, it significantly impairs synoviocyte migration, a critical process in pannus formation and joint destruction. Together, these data support a multi-modal mechanism through which brepocitinib counteracts RA pathophysiology, providing mechanistic insight into its therapeutic potential and setting the stage for further in vivo validation.

2. Objectives

In this study, we comprehensively characterized the effects of brepocitinib on MH7A synoviocytes to explore its potential targets in the treatment of RA.

3. Methods

3.1. Reagents and Cell Line

Brepocitinib (PF-06700841), a selective TYK2/JAK1 inhibitor, was obtained from Selleck Chemicals and prepared as a 10 mM stock solution in DMSO. Additional reagents including MTT solution, TRIzol, SYBR Green PCR master mix, cDNA synthesis kit, and enhanced chemiluminescence (ECL) substrate were purchased from Thermo Fisher Scientific. ELISA kits specific for human IL-6, TNF-α, and IFN-γ were obtained from R&D systems. Primary antibodies against p-TYK2, TYK2, p-JAK1, JAK1, p-STAT1, STAT1, p-STAT3, STAT3, BAX, BCL-2, cleaved caspase-3, total caspase-3, and GAPDH were purchased from cell signaling technology.

MH7A cells, a human RA synoviocyte line, were cultured in Dulbecco's Modified Eagle Medium (DMEM) supplemented with 10% fetal bovine serum (FBS) and 1% penicillin-streptomycin. Cells were maintained at 37°C in a humidified atmosphere of 5% CO_2. Cells were treated with brepocitinib at final concentrations of 0.5 μM, 1 μM, or 5 μM. DMSO was used as the vehicle control at a consistent concentration of 0.1% in all groups. For clarity, these concentrations are referred to throughout the manuscript as low (0.5 μM), medium (1 μM), and high (5 μM) doses.

Primary RA fibroblast-like synoviocytes (RA-FLS; HFLS-RA, Cell Applications, Cat. No. 408RA-05a) were cultured according to the supplier's instructions in Synoviocyte growth medium (Cell Applications, Cat. No. 415-500). Cells were maintained at 37°C in 5% CO_2 and used between passages 3 - 6 to ensure phenotypic stability. RA-FLS were treated with brepocitinib at the same concentrations (0.5, 1, 5 μM, 24 h) for dose-response experiments, or with 1 μM brepocitinib for time-course experiments (0, 30, 60, 240 min, and 24 h). Tofacitinib (1 μM; Selleck Chemicals) was included as a pharmacological comparator in selected experiments.

Brepocitinib was tested at 0.5, 1, and 5 μM, concentrations selected based on previously reported pharmacokinetic data showing that therapeutic plasma exposures in clinical studies fall within the low micromolar range (C-max ~1 - 2 μM). Thus, our experimental range encompasses clinically relevant

concentrations while allowing assessment of dose–response relationships (13, 14).

3.2. Cell Viability Assay

To evaluate cytotoxicity, the MTT [3-(4,5-dimethylthiazol-2-yl)-2,5-diphenyltetrazolium bromide] assay was performed using MH7A cells seeded in 96-well plates at a density of 10,000 cells per well. After 24 hours of brepocitinib treatment, 10 µL of MTT reagent (5 mg/mL) was added and MTT was performed (15).

3.3. Western Blotting

For protein analysis, MH7A cells were lysed using RIPA buffer supplemented with protease and phosphatase inhibitors. Protein concentrations were determined using the bicinchoninic acid (BCA) method. Equal amounts of protein (30 µg) were separated by SDS-PAGE, transferred, and blotted as described (13-15). Primary antibodies were obtained from cell signaling technology (CST; catalog numbers: p-TYK2 #9321, TYK2 #14193, p-JAK1 #3331, JAK1 #3344, p-STAT1 #7649, STAT1 #14994, p-STAT3 #9145, STAT3 #12640, BAX #2772, BCL-2 #4223, cleaved caspase-3 #9664, caspase-3 #9662, GAPDH #5174). GAPDH was used as a loading control. Blots were developed using ECL substrate (Thermo Fisher) and imaged on a Bio-Rad ChemiDoc system. Densitometric quantification was performed using ImageJ, with band intensities normalized to GAPDH and expressed as relative fold-change compared with vehicle control. For time-course experiments, primary RA-FLS (HFLS-RA) were treated with brepocitinib (1 µM) and harvested at 15, 30, 60, 240 minutes, and 24 hours. Western blotting was performed for p-STAT1, STAT1, p-STAT3, and STAT3 to evaluate the kinetics of signaling inhibition.

3.4. Quantitative PCR

Total RNA was extracted from MH7A cells using TRIzol reagent, and their cDNAs were synthesized from 1 µg of RNA using a reverse transcription kit. Real-time PCR was conducted as previously described (13). Each reaction was run in triplicate, and relative gene expression was calculated using the $2^{-\Delta\Delta Ct}$ method with GAPDH as the reference gene. Primer sequences for IL-6, TNF-α, IFN-γ, and GAPDH are provided in Appendix 1 in Supplementary File. Results are reported as mean fold-change ± SD from at least three independent experiments.

3.5. Enzyme-Linked Immunosorbent Assay

Supernatants from MH7A cells were collected after 24-hour treatment and analyzed for cytokine concentrations using ELISA kits for IL-6, TNF-α, and IFN-γ according to the manufacturer's instructions. Absorbance was measured at 450 nm, and cytokine levels were calculated based on the standard generated curves. Values were expressed in pg/mL and normalized to total protein content. Each condition was assayed in triplicate per experiment, with three independent biological replicates. Results are expressed as pg/mL normalized to total protein content and reported as mean ± SD.

3.6. Apoptosis Analysis

Apoptosis was evaluated by examining BAX/BCL-2 protein ratios and cleaved caspase-3 expression using Western blot. MH7A cells were treated with brepocitinib (0.5, 1, or 5 µM) for 24 hours, lysed, and analyzed for apoptotic markers. Densitometry was performed using ImageJ, and the BAX/BCL-2 ratio was calculated as normalized band intensities. Cleaved caspase-3 was expressed as a percentage relative to total caspase-3 protein. As a positive control, MH7A cells were treated with doxorubicin (1 µM, 24 h), a well-established apoptosis inducer via DNA damage and mitochondrial pathway activation, to validate assay sensitivity. This ensured that brepocitinib-induced effects could be distinguished from non-specific cytotoxic responses.

3.7. Wound Healing Assay

MH7A cells were seeded in 6-well plates and cultured to confluence. A linear scratch was made using a sterile 200 µL pipette tip, and debris was removed by washing with phosphate-buffered saline (PBS). Cells were treated with brepocitinib in serum-free medium. Images were taken at 0 h and 24 h using a phase-contrast microscope. Wound closure was quantified by two independent blinded investigators using ImageJ, with closure percentage calculated as: A lower wound closure percentage indicates reduced migratory capacity of synoviocytes. Three independent experiments were performed, each with duplicate wells per condition.

Equation 1.

$$\text{Wound closure}\left(\%\right) = \frac{Area_{0h} - Area_{24h}}{Area_{24h}} \quad (1)$$

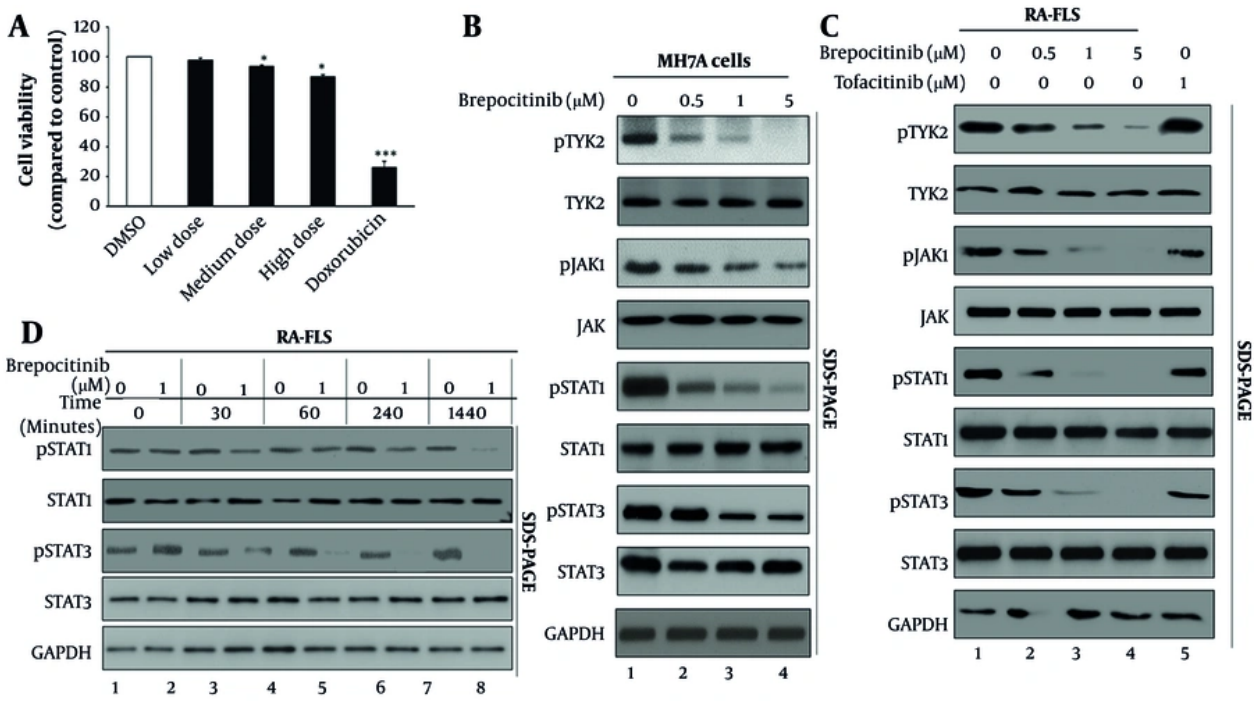

Figure 1. Effects of brepocitinib on MH7A cell viability and JAK-STAT pathway activation. A, cell viability of MH7A synoviocytes following treatment with brepocitinib at concentrations of 0.5 μM, 1 μM, and 5 μM for 24 hours. MTT assay was performed, and absorbance at 570 nm was normalized to DMSO control (0.1%). Data represent mean ± SD from three independent experiments. * $P < 0.05$ vs. vehicle. Although small statistical differences were detected at 1 μM and 5 μM, all brepocitinib-treated groups maintained viability above the predefined non-cytotoxic threshold (≥ 85% of vehicle). Therefore, these changes are considered not biologically relevant and confirm that brepocitinib is non-cytotoxic within the tested range. doxorubicin (1 μM) was used as a positive control and showed a marked reduction (~20%) in viability, validating assay responsiveness. B, brepocitinib suppresses phosphorylation of JAK-STAT pathway proteins in MH7A synoviocytes. MH7A cells were treated with brepocitinib at concentrations of 0.5 μM, 1 μM, and 5 μM for 24 hours. Western blot analysis was performed to assess the expression of phosphorylated and unphosphorylated forms of TYK2, JAK1, STAT1, and STAT3. GAPDH was used as a loading control. Protein lysates (30 μg per lane) were resolved by SDS-PAGE and probed with specific antibodies as indicated. Blots are representative of three independent experiments. Regression analysis confirmed a significant concentration-dependent reduction in p-JAK1 and p-STAT3 ($R^2 > 0.90$, $P < 0.01$). C, validation in primary RA-FLS (HFLS-RA). Cells were treated with brepocitinib (0.5, 1, 5 μM, 24 h) or tofacitinib (1 μM) and analyzed by Western blot for p-TYK2, TYK2, p-JAK1, JAK1, p-STAT1, STAT1, p-STAT3, and STAT3. GAPDH served as loading control. Results represent mean ± SD from three independent experiments. Low, medium, and high doses correspond to 0.5, 1, and 5 μM brepocitinib, respectively. Regression analysis also confirmed dose-dependent suppression of p-TYK2, p-JAK1, p-STAT1, and p-STAT3 in RA-FLS ($R^2 > 0.88$, $P < 0.01$). D, primary RA-FLS (HFLS-RA) were treated with brepocitinib (1 μM) for 0, 30, 60, 240 minutes, and 24 hours. Western blot analysis was performed for p-STAT1, STAT1, p-STAT3, and STAT3, with GAPDH serving as the loading control. Values represent mean ± SD from at least three independent experiments. Significance compared with control: * $P < 0.05$, *** $P < 0.001$. Two-way ANOVA demonstrated significant effects of treatment, time, and their interaction ($P < 0.05$). In all experiments, low, medium, and high doses correspond to 0.5 μM, 1 μM, and 5 μM brepocitinib, respectively.

3.8. Statistical Analysis

All data are presented as mean ± standard deviation (SD) from at least three independent experiments. Statistical significance was determined by one-way analysis of variance (ANOVA) followed by Tukey's multiple comparison test. For cytokine analyses across multiple groups, corrections for multiple comparisons were applied (Bonferroni). For dose–response experiments, regression analysis was used to confirm concentration-dependent trends. Two-way ANOVA was applied to time-course experiments to test for interaction between time and treatment. * $P < 0.05$, ** $P < 0.01$, * $P < 0.001$ were considered statistically significant.

4. Results

4.1. Brepocitinib Is Non-cytotoxic at Therapeutically Relevant Concentrations in MH7A Synoviocytes

To determine non-cytotoxic concentrations of brepocitinib, MH7A synoviocytes were treated with 0.5 μM, 1 μM, and 5 μM for 24 hours, followed by MTT assay. As shown in Figure 1A, all tested concentrations maintained cell viability above 85%. We prospectively defined ≥ 85% of the vehicle signal as the non-cytotoxic threshold for MH7A cells. Although small reductions at 1

μM and 5 μM reached statistical significance, the effect sizes were modest (≤ 10 - 15% vs vehicle) and remain within this predefined non-cytotoxic range. Because MTT primarily reflects mitochondrial reductase activity, such small statistical differences indicate assay sensitivity and metabolic modulation rather than overt cell death. By contrast, the doxorubicin positive control reduced viability to ~20% (confirming assay responsiveness), which we consider a biologically meaningful toxic effect. These results establish that brepocitinib, up to 5 μM, does not produce biologically relevant cytotoxicity over 24 h, and that subsequent experiments using these concentrations reflect specific pharmacological effects rather than nonspecific toxicity.

4.2. Brepocitinib Inhibits JAK-STAT Signaling in a Dose-Dependent Manner

Having established a safe and therapeutically relevant dose range, we next investigated whether brepocitinib effectively inhibits the JAK-STAT pathway, a key mediator of inflammatory signaling in RA synoviocytes. Western blot analysis (Figure 1B) revealed a dose-dependent suppression of phosphorylated TYK2, JAK1, STAT1, and STAT3 after 24-hour treatment. Notably, phosphorylation levels of p-JAK1 and p-STAT3 were reduced by over 80% at 5 μM brepocitinib, while total protein levels of each target remained unchanged, indicating specific inhibition of pathway activation. This confirms brepocitinib's direct effects on the intracellular signaling of MH7A cells.

To validate these findings in a more physiologically relevant context, primary RA-FLS (HFLS-RA) were analyzed under identical conditions (Figure 1C). Brepocitinib again produced a dose-dependent reduction in p-TYK2, p-JAK1, p-STAT1, and p-STAT3 (45 - 80% inhibition at 1 - 5 μM), while total protein expression was unaffected. In contrast, tofacitinib (1 μM) significantly inhibited JAK1 and STAT3 phosphorylation but showed minimal effects on TYK2, confirming differential selectivity. These results demonstrate that brepocitinib's dual TYK2/JAK1 blockade is preserved in primary RA synoviocytes and can be benchmarked against an established JAK inhibitor. Regression analysis again confirmed a significant dose-dependent suppression of p-TYK2, p-JAK1, p-STAT1, and p-STAT3 ($R^2 > 0.88$, $P < 0.01$).

To further assess the temporal dynamics of pathway inhibition, RA-FLS were treated with brepocitinib (1 μM) and harvested at 0, 30, 60, 240 minutes, and 24 hours (Figure 1D). Western blotting showed a rapid decline in p-STAT1 and p-STAT3 within 30 minutes, reaching maximal suppression by 60 minutes (~85% reduction), with inhibition largely sustained through 24 hours. Total STAT1 and STAT3 levels remained unchanged across all timepoints, indicating that brepocitinib exerts a rapid and durable blockade of downstream signaling. Two-way ANOVA demonstrated significant effects of treatment, time, and their interaction ($P < 0.05$).

4.3. Brepocitinib Reduces Pro-inflammatory Cytokine Expression at Both mRNA and Protein Levels

To assess downstream functional outcomes of JAK-STAT inhibition, we measured the expression of key inflammatory cytokines, IL-6, TNF-α, and IFN-γ, at both the mRNA and protein levels. QPCR analysis showed significant, dose-dependent downregulation of all three cytokine mRNAs (Figure 2A). At 5 μM, IL-6 and TNF-α transcript levels were reduced by over 80%, while IFN-γ mRNA was suppressed by 70%. To confirm the inhibitory effects of JAK-STAT blockade in synovial fibroblasts, we assessed mRNA expression of inflammatory cytokines in RA-FLS. QPCR analysis revealed a clear dose-dependent suppression of IL-6, TNF-α, and IFN-γ mRNA following brepocitinib treatment (Figure 2B). At 1 μM, IL-6, TNF-α, and IFN-γ levels were reduced by approximately 25 - 35% compared to control. At 5 μM, IL-6 and TNF-α expression declined by nearly 50%, while IFN-γ decreased by ~35%. At 10 μM, IL-6 levels were suppressed by over 75%, TNF-α expression was reduced by more than 90%, and IFN-γ decreased by nearly 70%. These findings closely parallel the MH7A data and highlight that brepocitinib robustly attenuates inflammatory cytokine production.

Correspondingly, ELISA results confirmed that brepocitinib markedly reduced cytokine secretion into the culture medium (Figure 2C). IL-6 protein levels decreased from 100 pg/mL in control to 20 pg/mL at 5 μM, and TNF-α levels dropped from 150 pg/mL to 15 pg/mL. ELISA confirmed that brepocitinib treatment significantly suppressed cytokine secretion into the culture supernatant of RA-FLS in a dose-dependent manner (Figure 2D). IL-6 protein levels decreased from ~96 pg/mL in control to 16 pg/mL at 5 μM. TNF-α secretion dropped from ~147 pg/mL in control cells to ~11 pg/mL at 5 μM. Similarly, IFN-γ levels were reduced from ~41 pg/mL to ~11 pg/mL. Statistical analysis with Bonferroni-corrected group comparisons confirmed significance for all three cytokines, and regression

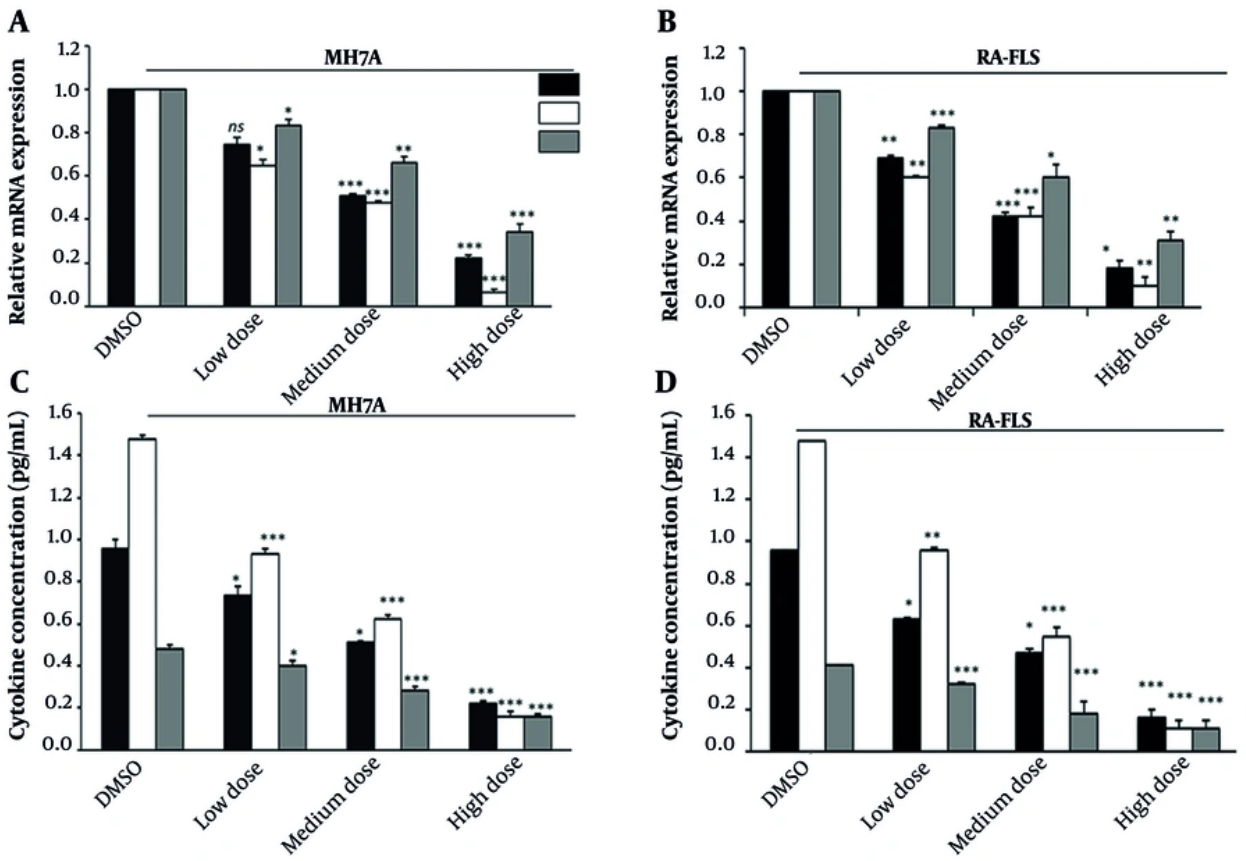

Figure 2. Analysis of pro-inflammatory cytokine expression in MH7A synoviocytes treated with brepocitinib. A, MH7A cells were treated with brepocitinib at concentrations of 0.5 μM, 1 μM, and 5 μM for 24 hours. Total RNA was extracted using TRIzol reagent, and cDNA was synthesized using a reverse transcription kit. B, RA-FLS cells were treated with brepocitinib at concentrations of 0.5 μM, 1 μM, and 5 μM for 24 hours. Total RNA was extracted using TRIzol reagent, and cDNA was synthesized using a reverse transcription kit. Quantitative real-time PCR (qPCR) was performed using SYBR Green master mix on a QuantStudio 5 thermocycler. Specific primers were used to detect IL-6, TNF-α, and IFN-γ transcripts, with GAPDH serving as the endogenous control. Relative mRNA expression was calculated using the $2^{-\Delta\Delta Ct}$ method and normalized to DMSO-treated control cells. Results represent the mean fold change from three independent experiments. C, cell culture supernatants of MH7A were collected from the same treatment groups after 24 hours and analyzed by enzyme-linked immunosorbent assay (ELISA). D, cell culture supernatants were collected from RA-FLS after 24 hours of brepocitinib treatment and analyzed by enzyme-linked immunosorbent assay (ELISA). Commercially available ELISA kits were used to quantify the concentrations of IL-6, TNF-α, and IFN-γ according to the manufacturers' protocols. Absorbance was measured at 450 nm using a microplate reader, and cytokine levels were interpolated from standard curves. Data were normalized to total protein content in each well. Results are shown as mean cytokine concentrations (pg/mL) from three independent experiments. Low, medium, and high doses correspond to 0.5, 1, and 5 μM brepocitinib, respectively. Values represent mean ± SD from at least three independent experiments. Significance compared with control: * $P < 0.05$, ** $P < 0.01$, *** $P < 0.001$. Bonferroni-corrected comparisons confirmed significance for all cytokines, and regression analysis supported dose-dependent suppression ($P < 0.01$). In all experiments, low, medium, and high doses correspond to 0.5 μM, 1 μM, and 5 μM brepocitinib, respectively.

analysis supported dose-dependent inhibition ($P < 0.01$). These results highlight that brepocitinib robustly diminishes the inflammatory cytokine milieu in RA synoviocytes at both transcript and protein levels.

4.4. Brepocitinib Modulates Apoptotic Pathways in MH7A Synoviocytes

Considering the apoptosis-resistant phenotype of RA synoviocytes, we investigated whether brepocitinib could restore pro-apoptotic signaling in MH7A cells. Western blot analysis (Figure 3A) revealed dose-dependent upregulation of the pro-apoptotic protein BAX and downregulation of the anti-apoptotic protein BCL-2, alongside a marked increase in the active cleaved form of caspase-3, with no significant change in total caspase-3 expression. These changes suggest activation of the intrinsic (mitochondrial) apoptotic pathway.

To quantify this effect, we calculated the BAX/BCL-2 ratio and the relative level of cleaved caspase-3, presented in Figure 3B. The BAX/BCL-2 ratio increased

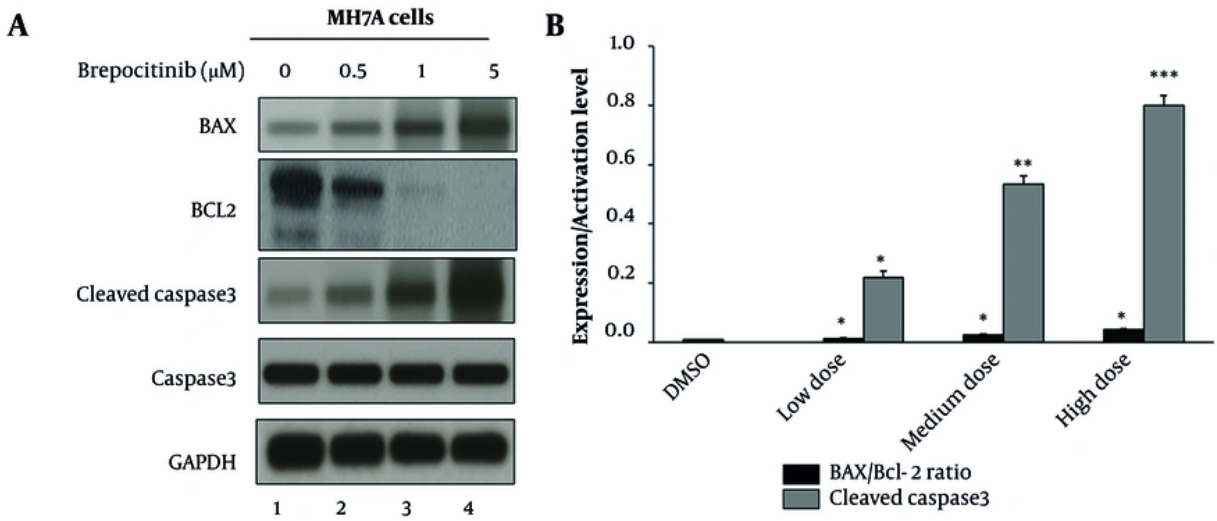

Figure 3. Evaluation of apoptotic markers in MH7A synoviocytes following brepocitinib treatment. A, MH7A cells were treated with brepocitinib at concentrations of 0.5 μM, 1 μM, and 5 μM for 24 hours. Total cellular protein was extracted using RIPA buffer containing protease inhibitors. Protein lysates (30 μg) were subjected to SDS-PAGE and transferred to PVDF membranes. Membranes were probed with antibodies specific to BAX, BCL-2, total caspase-3, and cleaved caspase-3. GAPDH was used as a loading control. Immunoreactive bands were visualized using enhanced chemiluminescence (ECL), and representative blots from three independent experiments are shown. B, densitometric analysis of Western blot bands was performed using ImageJ software. The ratio of BAX to BCL-2 protein expression was calculated as an indicator of pro-apoptotic signaling. Cleaved caspase-3 levels were quantified relative to total caspase-3 and expressed as a percentage. Data represent the mean ± SD from three independent experiments. Low, medium, and high doses correspond to 0.5, 1, and 5 μM brepocitinib, respectively. Values represent mean ± SD from at least three independent experiments. Significance compared with control: * $P < 0.05$, ** $P < 0.01$, *** $P < 0.001$. In all experiments, low, medium, and high doses correspond to 0.5 μM, 1 μM, and 5 μM brepocitinib, respectively.

progressively with increasing dose, from 1.0 in DMSO control to 4.0 at 5 μM brepocitinib, indicating a shift toward pro-apoptotic signaling. In parallel, cleaved caspase-3 levels reached 80% of the maximal response. These findings confirm that brepocitinib promotes apoptosis in MH7A synoviocytes by rebalancing BCL-2 family protein expression and activating the caspase cascade, thereby counteracting the hyperplastic, apoptosis-resistant phenotype typical of RA synovium.

4.5. Brepocitinib Inhibits Synoviocyte Migration

To further explore brepocitinib's functional impact, particularly its relevance to joint invasion and pannus formation in RA, we performed a wound healing assay to measure synoviocyte migration. MH7A monolayers treated with increasing concentrations of brepocitinib displayed a dose-dependent reduction in wound closure at 24 hours (Figure 4A). Using the corrected formula (shown in materials and methods), DMSO controls closed approximately 75% of the wound, whereas brepocitinib reduced closure to ~55% (0.5 μM), ~40% (1 μM), and ~20% (5 μM) (Figure 4B). Importantly, these anti-migratory effects occurred under serum-free conditions and in the absence of biologically relevant cytotoxicity (confirmed in Figure 1A), indicating that brepocitinib specifically impairs cell motility. Statistical analysis was performed using one-way ANOVA followed by Tukey's multiple comparison test, and significance was indicated in Figure 4B. Regression analysis confirmed a significant linear relationship between concentration and inhibition of wound closure ($R^2 > 0.95$, $P < 0.01$). This adds a key dimension to its anti-RA potential by limiting the invasive behavior of synoviocytes.

4.6. A Summary Model Highlights the Integrated Mechanisms of Brepocitinib Action

To synthesize the molecular and functional effects observed across our experimental results, we constructed a mechanistic summary diagram (Figure 5). The model illustrates how brepocitinib binds and inhibits TYK2 and JAK1, blocking downstream STAT1/3 phosphorylation. This results in the downregulation of inflammatory cytokines (IL-6, TNF-α, IFN-γ), leading to reduced inflammation and impaired synoviocyte migration, while simultaneously tipping the

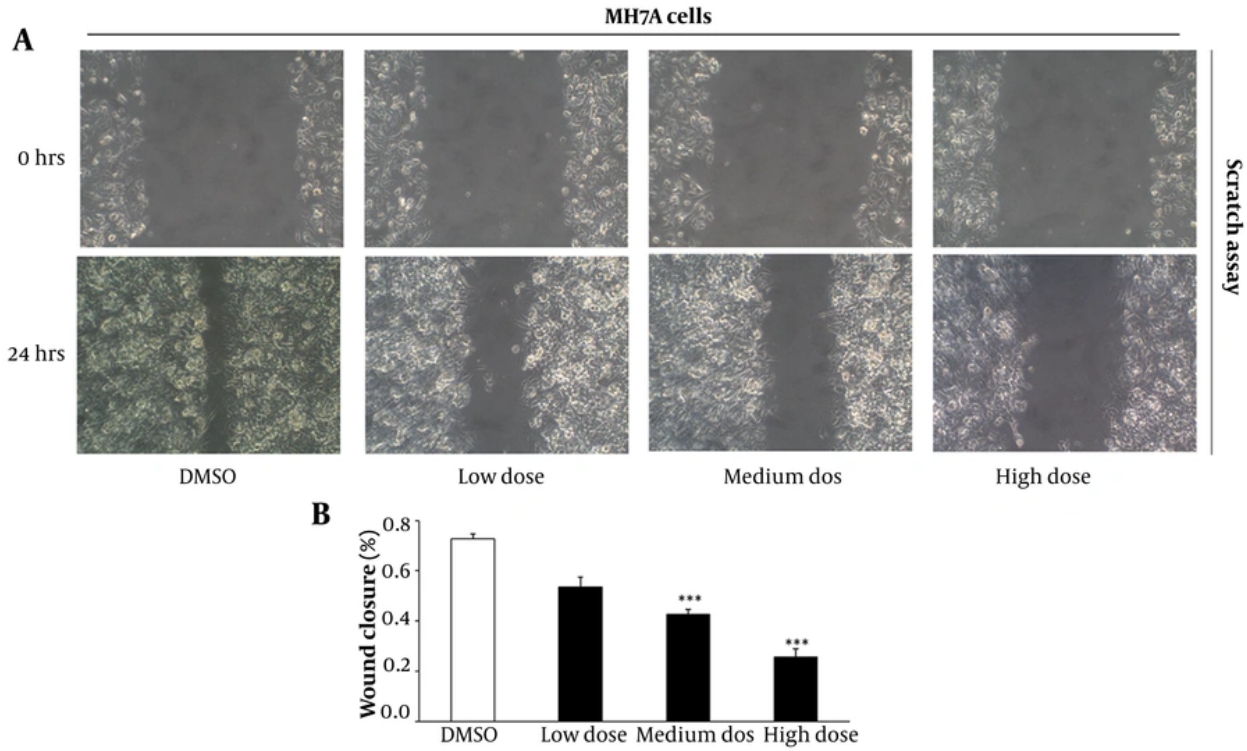

Figure 4. Assessment of MH7A synoviocyte migration using wound healing assay after brepocitinib treatment. A, MH7A synoviocytes were cultured to confluence in 6-well plates and treated with brepocitinib at concentrations of 0.5 μM, 1 μM, and 5 μM, or with 0.1% DMSO as vehicle control. A linear scratch ("wound") was introduced using a sterile 200 μL pipette tip, and wells were washed with PBS to remove detached cells. Cells were incubated in serum-free medium containing the indicated treatments. Phase-contrast images were taken at 0 and 24 hours using an inverted microscope to monitor wound closure. B, quantification of wound closure was performed using ImageJ software. Wound area at 0 and 24 hours was measured for each treatment group, and percentage closure was calculated using the Equation 1. Data represent the mean ± SD from three independent experiments. Low, medium, and high doses correspond to 0.5, 1, and 5 μM brepocitinib, respectively. Values represent mean ± SD from at least three independent experiments. Significance compared with control: * $P < 0.05$, ** $P < 0.01$, *** $P < 0.001$. Regression analysis confirmed a significant linear relationship between concentration and inhibition of wound closure ($R^2 > 0.95$, $P < 0.01$). In all experiments, low, medium, and high doses correspond to 0.5 μM, 1 μM, and 5 μM brepocitinib, respectively.

intracellular balance toward apoptosis (via increased BAX/BCL-2 ratio and caspase-3 activation). Together, these data reveal that brepocitinib exerts multi-faceted therapeutic effects against synovial pathology in RA.

5. Discussion

Cancer, autoimmune disorders, and infectious diseases continue to impose a significant global health burden, contributing to chronic disability, reduced quality of life, and escalating healthcare costs (16-20). Among these, RA is marked by chronic synovial inflammation, immune dysregulation, and pathological remodeling of the joint environment (1, 2). Although current JAK inhibitors have advanced RA treatment, their limited selectivity and associated adverse effects underscore the need for more targeted therapeutics. In this study, we systematically evaluated the molecular and cellular effects of brepocitinib, a dual TYK2/JAK1 inhibitor, in MH7A synoviocytes, which serve as an established in vitro model for human RA pathogenesis.

Our results demonstrate that brepocitinib exerts a multi-dimensional profile by inhibiting inflammatory signaling, suppressing cytokine expression, promoting apoptosis, and impairing synoviocyte migration — four hallmarks of RA pathology. These findings are consistent with earlier preclinical and clinical observations in psoriatic arthritis, lupus, and hidradenitis suppurativa, where brepocitinib showed robust immunomodulatory activity (12, 13).

We first confirmed that brepocitinib is non-cytotoxic at concentrations up to 5 μM in MH7A cells, allowing downstream effects to be attributed to targeted

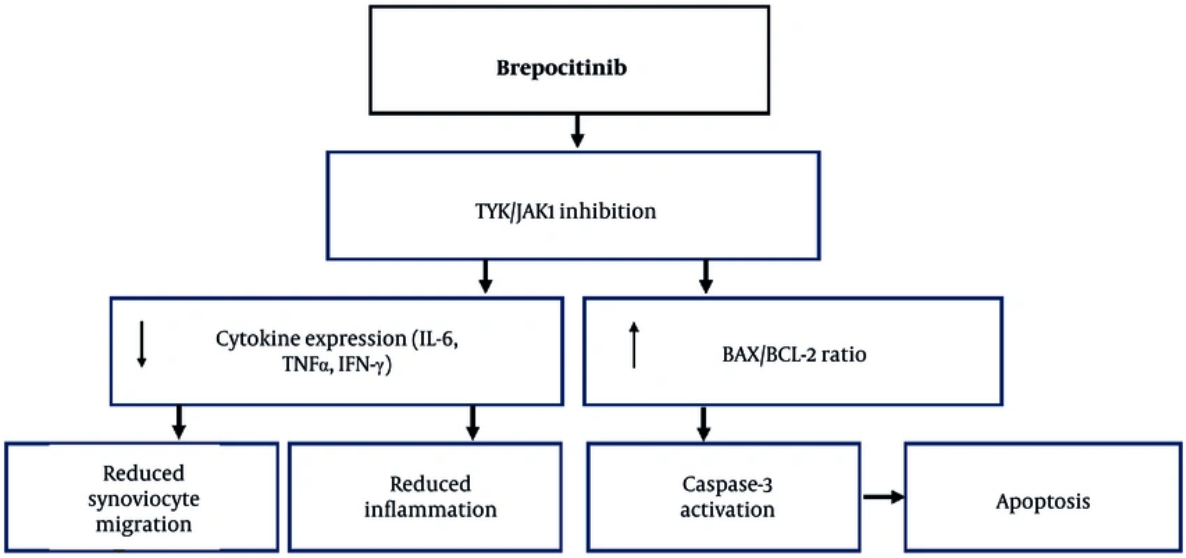

Figure 5. Mechanistic summary of brepocitinib's molecular and functional effects in MH7A synoviocytes. This diagram synthesizes findings from Figures 1 - 4 into an integrated pathway model of brepocitinib action. The illustration highlights brepocitinib's dual inhibition of TYK2 and JAK1, leading to downstream suppression of STAT1 and STAT3 phosphorylation. These upstream effects result in reduced transcription and secretion of key inflammatory cytokines (IL-6, TNF-α, and IFN-γ), which in turn drive reduced inflammation and impaired synoviocyte migration. Simultaneously, brepocitinib promotes mitochondrial-dependent apoptosis via increased BAX/BCL-2 ratio and activation of caspase-3. Notably, the inhibition of migration is independent of apoptosis, reflecting a cytokine-driven mechanism rather than loss of cell viability.

pathway inhibition rather than nonspecific toxicity. Mechanistically, brepocitinib inhibited JAK-STAT signaling, evidenced by reduced phosphorylation of TYK2, JAK1, STAT1, and STAT3, in agreement with prior studies identifying these kinases as central to IL-6 and interferon signaling (21). The dual targeting profile distinguishes brepocitinib from existing JAK inhibitors and may provide broader pathway coverage while minimizing JAK2-related hematologic effects.

To extend translational relevance, we validated these findings in primary RA-FLS (HFLS-RA). Brepocitinib produced dose-dependent inhibition of TYK2, JAK1, STAT1, and STAT3 phosphorylation in RA-FLS, paralleling MH7A responses. Benchmarking against tofacitinib highlighted broader suppression by brepocitinib, since tofacitinib primarily inhibited JAK1/STAT3 but not TYK2. These results demonstrate that brepocitinib's molecular effects are preserved in primary synoviocytes and underscore the potential advantage of dual TYK2/JAK1 inhibition.

This upstream blockade translated into robust suppression of IL-6, TNF-α, and IFN-γ at both transcript and protein levels. IL-6, in particular, is directly regulated via JAK1/STAT3 and is a validated therapeutic target (22). The observed reductions indicate that brepocitinib effectively downregulates the inflammatory milieu that drives synovial pathology.

In addition, brepocitinib modulated apoptosis-related proteins by increasing BAX, decreasing BCL-2, and activating caspase-3, thereby restoring pro-apoptotic signaling in apoptosis-resistant synoviocytes. This is consistent with prior evidence that JAK-STAT inhibition can counteract survival signaling in RA-FLS (23). Functionally, brepocitinib reduced synoviocyte migration in wound-healing assays, suggesting interference with invasive behavior relevant to pannus formation.

We acknowledge, however, that the wound-healing assay has inherent limitations, including potential influence from proliferation. To minimize bias, assays were conducted under serum-free conditions, with blinded image analysis and replicate independent experiments. Nevertheless, we did not employ complementary methods such as transwell migration or 3D cultures, which would provide additional physiological validation. Future studies will extend to

these platforms to further confirm migratory inhibition.

The final mechanistic model (Figure 5) summarizes brepocitinib's effects, linking TYK2/JAK1 inhibition to downstream STAT1/3 deactivation, reduced cytokine output, restoration of apoptosis, and impaired migration. These systems-level effects provide mechanistic insight into how dual TYK2/JAK1 blockade can counter synovial pathology.

It is important to note several limitations. The work was conducted in vitro using MH7A cells and RA-FLS monocultures, which cannot fully capture the complexity of synovial tissue or mixed cell populations in vivo. Rescue experiments, such as STAT overexpression, were not performed and would further strengthen mechanistic claims. Additionally, systemic effects and toxicities were not assessed, and future studies incorporating animal models or patient-derived tissues are needed to confirm therapeutic applicability. We also did not conduct independent kinase-profiling under our experimental conditions; however, published kinase panel studies demonstrate that brepocitinib inhibits TYK2 and JAK1 with nanomolar potency while sparing JAK2, JAK3, and most non-JAK kinases (10), supporting the specificity of our findings.

Overall, these results provide mechanistic insights into brepocitinib's cellular effects in RA synoviocytes and generate hypotheses for further preclinical validation. While our data highlight key pathways and functions disrupted by dual TYK2/JAK1 inhibition, additional in vivo studies are required before definitive therapeutic conclusions can be drawn.

5.1. Conclusions

Brepocitinib displays potent anti-inflammatory, pro-apoptotic, and anti-migratory effects in MH7A synoviocytes via dual inhibition of the TYK2 and JAK1 pathways. These findings validate its mechanistic action in RA and support its potential as a targeted therapeutic agent that not only suppresses inflammation but also addresses synovial hyperplasia and joint destruction.

Supplementary Material

Supplementary material(s) is available here [To read supplementary materials, please refer to the journal website and open PDF/HTML].

Footnotes

AI Use Disclosure: The authors declare that no generative AI tools were used in the creation of this article.

Authors' Contribution: Study concept and design: U. S. and Z. Z. P.; Acquisition of data: Z. Z. P. and U. S.; Analysis and interpretation of data: U. S., Z. Z. P., A. M. N., and S. M. N.; Drafting of the manuscript: U. S. and Z. Z. P.; Critical revision of the manuscript for important intellectual content: S. M. N., A. M. N., and U. S.; Statistical analysis: U. S. and Z. Z. P.; Administrative, technical, and material support: Z. Z. P. and U. S.; Study supervision: U. S. and S. M. N.

Conflict of Interests Statement: The authors do not declare any conflicts of interest for this study.

Data Availability: The dataset presented in the study is available on request from the corresponding author.

Ethical Approval: This study is approved under the ethical approval 31202008 of International Center of Medical Sciences Research (ICMSR), Austin, TX, United States; ICMSR-Essex, United Kingdom; ICMSR-Islamabad, Pakistan.

Funding/Support: This study was supported by International Center of Medical Sciences Research (ICMSR), Austin, TX, United States; ICMSR-Essex, United Kingdom; ICMSR-Islamabad, Pakistan

References

1. Schuerwegh AJ, Ioan-Facsinay A, Dorjee AL, Roos J, Bajema IM, van der Voort EI, et al. Evidence for a functional role of IgE anticitrullinated protein antibodies in rheumatoid arthritis. *Proc Natl Acad Sci USA*. 2010;**107**(6):2586-91. [PubMed ID: 20133791]. [PubMed Central ID: PMC2823893]. https://doi.org/10.1073/pnas.0913054107.
2. Hunter TM, Boytsov NN, Zhang X, Schroeder K, Michaud K, Araujo AB. Prevalence of rheumatoid arthritis in the United States adult population in healthcare claims databases, 2004-2014. *Rheumatol Int*. 2017;**37**(9):1551-7. [PubMed ID: 28455559]. https://doi.org/10.1007/s00296-017-3726-1.
3. Bartok B, Firestein GS. Fibroblast-like synoviocytes: key effector cells in rheumatoid arthritis. *Immunol Rev*. 2010;**233**(1):233-55. [PubMed ID: 20193003]. [PubMed Central ID: PMC2913689]. https://doi.org/10.1111/j.0105-2896.2009.00859.x.
4. Pap T, Dankbar B, Wehmeyer C, Korb-Pap A, Sherwood J. Synovial fibroblasts and articular tissue remodelling: Role and mechanisms. *Semin Cell Dev Biol*. 2020;**101**:140-5. [PubMed ID: 31956018]. https://doi.org/10.1016/j.semcdb.2019.12.006.

5. Bottini N, Firestein GS. Duality of fibroblast-like synoviocytes in RA: passive responders and imprinted aggressors. *Nat Rev Rheumatol*. 2013;**9**(1):24-33. [PubMed ID: 23147896]. [PubMed Central ID: PMC3970924]. https://doi.org/10.1038/nrrheum.2012.190.
6. Wang Z, Wang J, Lan T, Zhang L, Yan Z, Zhang N, et al. Role and mechanism of fibroblast-activated protein-alpha expression on the surface of fibroblast-like synoviocytes in rheumatoid arthritis. *Front Immunol*. 2023;**14**:1135384. [PubMed ID: 37006278]. [PubMed Central ID: PMC10064071]. https://doi.org/10.3389/fimmu.2023.1135384.
7. Agashe RP, Lippman SM, Kurzrock R. JAK: Not Just Another Kinase. *Mol Cancer Ther*. 2022;**21**(12):1757-64. [PubMed ID: 36252553]. [PubMed Central ID: PMC10441554]. https://doi.org/10.1158/1535-7163.MCT-22-0323.
8. Fensome A, Ambler CM, Arnold E, Banker ME, Brown MF, Chrencik J, et al. Dual Inhibition of TYK2 and JAK1 for the Treatment of Autoimmune Diseases: Discovery of ((S)-2,2-Difluorocyclopropyl)((1 R,5 S)-3-(2-((1-methyl-1 H-pyrazol-4-yl)amino)pyrimidin-4-yl)-3,8-diazabicyclo[3.2.1]octan-8-yl)methanone (PF-06700841). *J Med Chem*. 2018;**61**(19):8597-612. [PubMed ID: 30113844]. https://doi.org/10.1021/acs.jmedchem.8b00917.
9. Traves PG, Murray B, Campigotto F, Galien R, Meng A, Di Paolo JA. JAK selectivity and the implications for clinical inhibition of pharmacodynamic cytokine signalling by filgotinib, upadacitinib, tofacitinib and baricitinib. *Ann Rheum Dis*. 2021;**80**(7):865-75. [PubMed ID: 33741556]. [PubMed Central ID: PMC8237188]. https://doi.org/10.1136/annrheumdis-2020-219012.
10. Paik JJ, Vencovský J, Charles-Schoeman C, Wright GC, Vleugels RA, Goriounova AS, et al. Brepocitinib, a potent and selective TYK2/JAK1 inhibitor: scientific and clinical rationale for dermatomyositis. *Clin Experim Rheumatol*. 2024. https://doi.org/10.55563/clinexprheumatol/eeglsa.
11. Kimball AB, Peeva E, Forman S, Moiin A, Khattri S, Porter ML, et al. Brepocitinib, Zimlovisertib, and Ropsacitinib in Hidradenitis Suppurativa. *NEJM Evid*. 2024;**3**(3):EVIDoa2300155. [PubMed ID: 38335032]. https://doi.org/10.1056/EVIDoa2300155.
12. Huang MY, Armstrong AW. Janus-kinase inhibitors in dermatology: A review of their use in psoriasis, vitiligo, systemic lupus erythematosus, hidradenitis suppurativa, dermatomyositis, lichen planus, lichen planopilaris, sarcoidosis and graft-versus-host disease. *Indian J Dermatol Venereol Leprol*. 2023;**90**(1):30-40. [PubMed ID: 38031699]. https://doi.org/10.25259/IJDVL_15_2023.
13. Dowty ME, Qiu R, Dantonio A, Niosi M, Doran A, Balesano A, et al. The Metabolism and Disposition of Brepocitinib in Humans and Characterization of the Formation Mechanism of an Aminopyridine Metabolite. *Drug Metab Dispos*. 2024;**52**(7):690-702. [PubMed ID: 38719744]. https://doi.org/10.1124/dmd.124.001750.
14. Maleki F, Chang C, Purohit VS, Nicholas T. Pharmacokinetic Profile of Brepocitinib with Topical Administration in Atopic Dermatitis and Psoriasis Populations: Strategy to Inform Clinical Trial Design in Adult and Pediatric Populations. *Pharm Res*. 2024;**41**(4):623-36. [PubMed ID: 38519816]. [PubMed Central ID: PMC11024034]. https://doi.org/10.1007/s11095-024-03654-w.
15. Saeed U, Piracha ZZ, Kwon H, Kim J, Kalsoom F, Chwae YJ, et al. The HBV Core Protein and Core Particle Both Bind to the PPiase Par14 and Par17 to Enhance Their Stabilities and HBV Replication. *Front Microbiol*. 2021;**12**:795047. [PubMed ID: 34970249]. [PubMed Central ID: PMC8713550]. https://doi.org/10.3389/fmicb.2021.795047.
16. Kocarnik JM, Compton K, Dean FE, Fu W, Gaw BL; Global Burden of Disease Cancer Collaboration, et al. Cancer Incidence, Mortality, Years of Life Lost, Years Lived With Disability, and Disability-Adjusted Life Years for 29 Cancer Groups From 2010 to 2019: A Systematic Analysis for the Global Burden of Disease Study 2019. *JAMA Oncol*. 2022;**8**(3):420-44. [PubMed ID: 34967848]. [PubMed Central ID: PMC8719276]. https://doi.org/10.1001/jamaoncol.2021.6987.
17. G. B. D. Colorectal Cancer Collaborators. Global, regional, and national burden of colorectal cancer and its risk factors, 1990-2019: a systematic analysis for the Global Burden of Disease Study 2019. *Lancet Gastroenterol Hepatol*. 2022;**7**(7):627-47. [PubMed ID: 35397795]. [PubMed Central ID: PMC9192760]. https://doi.org/10.1016/S2468-1253(22)00044-9.
18. Pharyngeal Cancer Collaborators, Compton K, Xu R, Mishra R; Gbd Lip Oral; Cunha, et al. The Global, Regional, and National Burden of Adult Lip, Oral, and Pharyngeal Cancer in 204 Countries and Territories: A Systematic Analysis for the Global Burden of Disease Study 2019. *JAMA Oncol*. 2023;**9**(10):1401-16. [PubMed ID: 37676656]. [PubMed Central ID: PMC10485745]. https://doi.org/10.1001/jamaoncol.2023.2960.
19. Gbd Lri Collaborators. Age-sex differences in the global burden of lower respiratory infections and risk factors, 1990-2019: results from the Global Burden of Disease Study 2019. *Lancet Infect Dis*. 2022;**22**(11):1626-47. [PubMed ID: 35964613]. [PubMed Central ID: PMC9605880]. https://doi.org/10.1016/S1473-3099(22)00510-2.
20. G. B. D. Upper Respiratory Infections Otitis Media Collaborators. Global, regional, and national burden of upper respiratory infections and otitis media, 1990-2021: a systematic analysis from the Global Burden of Disease Study 2021. *Lancet Infect Dis*. 2025;**25**(1):36-51. [PubMed ID: 39265593]. [PubMed Central ID: PMC11680489]. https://doi.org/10.1016/S1473-3099(24)00430-4.
21. Mease P, Helliwell P, Silwinska-Stanczyk P, Miakisz M, Ostor A, Peeva E, et al. Efficacy and Safety of the TYK2/JAK1 Inhibitor Brepocitinib for Active Psoriatic Arthritis: A Phase IIb Randomized Controlled Trial. *Arthritis Rheumatol*. 2023;**75**(8):1370-80. [PubMed ID: 37194394]. https://doi.org/10.1002/art.42519.
22. Huang B, Lang X, Li X. The role of IL-6/JAK2/STAT3 signaling pathway in cancers. *Front Oncol*. 2022;**12**:1023177. [PubMed ID: 36591515]. [PubMed Central ID: PMC9800921]. https://doi.org/10.3389/fonc.2022.1023177.
23. Salakou S, Kardamakis D, Tsamandas AC, Zolota V, Apostolakis E, Tzelepi V, et al. Increased Bax/Bcl-2 ratio up-regulates caspase-3 and increases apoptosis in the thymus of patients with myasthenia gravis. *In Vivo*. 2007;**21**(1):123-32. [PubMed ID: 17354625].